Journal of Biomechanics 94 (2019) 147–157

Contents lists available at ScienceDirect

Journal of Biomechanics

journal homepage: www.elsevier.com/locate/jbiomech
www.JBiomech.com

In vitro analysis of kinematics and elastostatics of the human rib cage during thoracic spinal movement for the validation of numerical models

Christian Liebsch [a], Nicolas Graf [a,b], Hans-Joachim Wilke [a,*]

[a] Institute of Orthopaedic Research and Biomechanics, Trauma Research Centre Ulm, Ulm University, Ulm, Germany
[b] SpineServ GmbH & Co. KG, Ulm, Germany

ARTICLE INFO

Article history:
Accepted 27 July 2019

Keywords:
Rib cage
Sternum
Kinematics
Bending deformation
In vitro study

ABSTRACT

Neither kinematic nor stiffness properties of the rib cage during thoracic spinal motion were investigated in previous studies, while being essential for the accurate validation of numerical models of the whole thorax. The aim of this in vitro study therefore was to quantify the kinematics and elastostatics of the human rib cage under defined boundary conditions. Eight fresh frozen human thoracic spine specimens (C7-L1, median age 55 years, ranging from 40 to 60 years) including entire rib cages were loaded quasi-statically in flexion/extension, lateral bending, and axial rotation using pure moments of 5 Nm. Relative motions of ribs, thoracic vertebrae, and sternal structures as well as strains on the ribs were measured using optical motion tracking of 150 reflective markers per specimen, while specimens were loaded displacement-controlled with a constant rate of 1°/s for 3.5 cycles. The third full cycle was used to determine relative angles and strains at full loading of the spine for all motion directions. Largest relative angles were found in the main loading directions with only small motions at the mid-thoracic levels. Highest strains of the intercostal spaces were detected in the anterior section of the lowest fourth of the rib cage, showing compressions and elongations of more than 10% in all spinal motion planes. Elastostatic rib deformation was generally less than 1%. Rib-sternum relative motions exhibited complex motion patterns, overall showing relative angles below 2°. The results indicate that rib cage structures are not macroscopically deformed during spinal motion, but exhibit characteristic reproducible kinematics patterns.

1. Introduction

The human rib cage represents a complex three-dimensional bony, cartilaginous, and ligamentous structure, serving as attachment point for various skeletal muscles of the upper body, as respiration support together with the intercostal muscles, and as protector of the inner organs. Previous studies showed that the rib cage furthermore functions as a stabilizer for the thoracic spine, especially during axial rotation movement (Watkins et al., 2005; Mannen et al., 2015a, 2015b; Liebsch et al., 2017a, 2017b). Therefore, its consideration in spinal in vitro testing as well as in numerical modelling of the thoracic spine is essential to ensure simulation of the best possible realistic spinal motion behaviour.

To achieve high model accuracy, kinematic and stiffness properties of all rib cage structures, determined under well-defined boundary conditions, are needed in order to validate finite element models as well as multi-body simulation models of the thoracic spine with articulated rib cage. Data on the complex mechanical behaviour of the human rib cage, however, are scarce, while previous studies specifically focused on rib cage stiffness during anterior-posterior loading with regard to its fracture toughness (Kindig et al., 2010) or rib cage kinematics during the respiration process (Beyer et al., 2016, 2017). To the authors' knowledge, however, there is no previous study investigating the three-dimensional rib cage kinematics and elastostatics during thoracic spinal movement.

The purpose of the present study therefore was to quantify the relative motions between (1) all ribs and their adjacent thoracic vertebrae, (2) all adjacent ribs, (3) ribs and sternum, and (4) the upper and lower sternum, as well as (5) the bending deformation of the ribs during three-dimensional thoracic spinal movements.

* Corresponding author at: Institute of Orthopaedic Research and Biomechanics, Helmholtzstraße 14, 89081 Ulm, Germany.
E-mail address: hans-joachim.wilke@uni-ulm.de (H.-J. Wilke).

https://doi.org/10.1016/j.jbiomech.2019.07.041
0021-9290/

2. Methods

2.1. Specimens

Eight fresh frozen specimens consisting of the entire thoracic spine (C7-L1), bony, cartilaginous, and ligamentous rib cage, and intercostal muscles were dissected from human torsos by carefully removing surrounding skin, fat, and muscle tissues. Specimens were screened for fractures and signs of severe degeneration using clinical CT scans (Somatom Definition AS, Siemens Healthcare, Erlangen, Germany) and visual inspection. Median donor age of the specimens was 55 years, ranging from 40 to 60 years, including one female and seven male donors. The same specimens were already used in a previous study investigating the effect of follower loading on the three-dimensional motion characteristics of the thoracic spine including the entire rib cage (Liebsch et al., 2018). Detailed information about the specimens' properties is given in this publication. C7 and L1 vertebrae were embedded half in PMMA (Technovit 3040, Heraeus Kulzer, Wehrheim, Germany), which was used to fix flanges for biomechanical testing. To enhance fixation of the vertebrae within the pottings, screws were driven into the vertebral bodies before embedding. Specimens were stored at −20 °C and thawed at 6 °C for about 12 h prior to preparation and testing. During testing, which was performed at room temperature, specimens were periodically moistened using 0.9% saline solution, while the total duration of preparation and testing was kept below 20 h to minimize the risk of specimen decomposition (Wilke et al., 1998).

2.2. Load application

Testing of the specimens was performed equivalent to previous in vitro studies investigating flexibility properties of the thoracic spine with entire rib cage (Liebsch et al., 2017a, 2017b, 2018). The specimens were loaded displacement-controlled with an angular velocity of 1°/s in flexion/extension, lateral bending, and axial rotation using a well-established spine tester (Wilke et al., 1994). Loading was performed quasi-statically by applying pure moments of 5 Nm in each motion direction, following recommendations for thoracic spinal in vitro testing (Wilke et al., 1998). In all motion planes, 3.5 loading cycles were applied, of which the third full cycle was used for data evaluation to minimize possible viscoelastic effects.

2.3. Optical motion tracking

For kinematic and elasto-static analysis of the rib cage structures during thoracic spinal loading, the optical motion capture system Vicon MX13 (Vicon Motion Systems Ltd., Oxford, UK) was used, consisting of 12 cameras surrounding the rib cage specimen. Specimens were equipped with 150 reflective markers in total, which were fixed to the bony structures via small screws (Fig. 1): 36 markers were placed on the thoracic spinous processes (three per vertebra, respectively, from T1 to T12), 108 markers on the ribs (three per rib of the 1st, 11th, and 12th rib level, respectively, and five per rib of the rib levels 2 to 10, respectively), and six markers on the sternum (three per upper and lower sternum, respectively). A number of at least three markers per bony structure was chosen to analyse three-dimensional relative motions of all adjacent bony structures by creating local coordinate systems of all single structures, while a number of five markers was used for the rib levels 2 to 10 to specifically detect relative macroscopic strains along as well as between the single ribs during thoracic spinal motion. Markers on the ribs were positioned posteriorly at the angulus costae and anteriorly at the front tip, while the remaining markers were distributed between these points along rib length. On each sternal section, two markers were placed superiorly and one marker inferiorly, while on the spinous processes, the markers were positioned horizontally, in order to create consistent axes of rotation for all specimens. In general, vertebrae and sternal structures were considered as fixed coordinate systems, around which motions of the rib coordinate systems were analysed, whereas in case of the analysis of relative motions between the two sternal structures (manubrium and body), the lower sternum was considered as fixed coordinate system during spinal loading. Preliminary tests on the accuracy of the test setup, where systematic errors and deviations of the parameters were quantified for predefined values and defined motions, exhibited a mean error value of <0.1° in rotational movements and <0.1 mm in translational movements, respectively.

Motion analysis was triggered by the start and stop signal of the spine tester, both measuring with a frequency of 50 Hz. To achieve highest possible accuracy by means of creating redundancies in the marker per camera ratio and due to the complex three-dimensional morphology of the rib cage, all specimens were tested in four different positions for each motion plane by turning the respective specimen 90° before each trial.

2.4. Data processing and evaluation

Three-dimensional relative motion data was post-processed using the software Nexus (Vicon Motion Systems Ltd., Oxford, UK), ensuring that every marker was tracked by at least three cameras. Motion and biomechanical loading data were merged using Matlab (MathWorks Inc., Natick, USA) and further processed using Microsoft Excel (Microsoft Corp., Redmond, USA). Three-dimensional relative deflections of the ribs and the upper sternum were determined at the point of full pure moment loading of 5 Nm for both respective spinal motion directions in each loading plane (flexion and extension, left and right lateral bending, left and right axial rotation). Inter- and intra-rib strains were evaluated using a custom-written Matlab script which determined the rib strains of the third spinal loading cycle relative to the unloaded state in each motion direction. Inter-rib strains were evaluated for the anteriorly, laterally, as well as posteriorly located markers. Intra-rib strains were defined as the strains between the markers of the specific rib and were determined between the anterior and posterior (global bending deformation) as well as between all adjoining markers (local bending deformation). Cumulative average deflections and strains of the eight specimens were calculated as medians and ranges.

2.5. Ethics

The use of human specimens was approved by the ethical committee board of the University of Ulm, Germany (No. 302/14) prior to experimental testing. Specimens were obtained from an accredited and ethically approved body donation program (Science Care Inc., Phoenix, Arizona, USA).

3. Results

3.1. Rib-vertebra relative motions

Deflections of the ribs relative to their adjacent vertebrae during spinal movement exhibited either symmetrical or inverse motion patterns depending on motion direction in all three motion planes (Figs. 2–4). In general, a transition zone of the motion ranges was detected at the levels T4 to T6, in which the relative

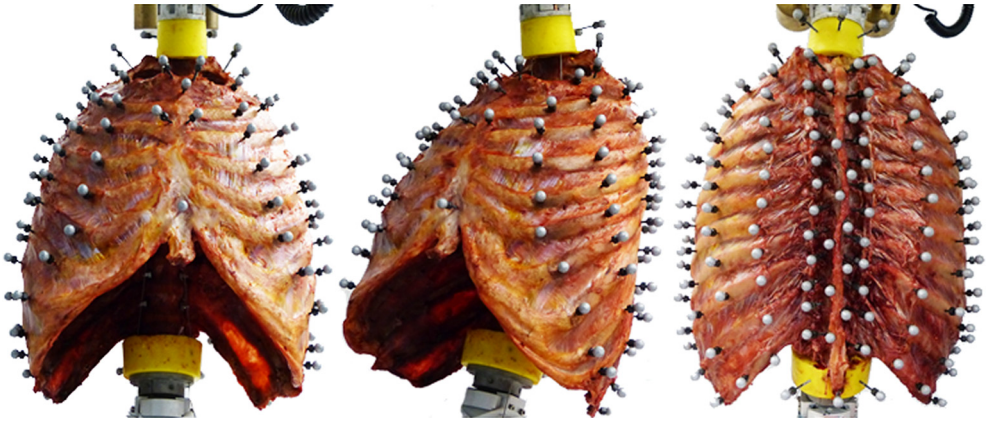

Fig. 1. Illustration of the marker setup for optical motion tracking of rib cage specimens: Three markers were fixed to the upper and lower sternum, 1st, 11th, and 12th ribs, as well as the spinous processes of the thoracic vertebrae, respectively. Five markers were fixed to each rib of the levels 2 to 10.

motions were distinctly lower and in which an inversion of the motion directions was seen.

In flexion and extension, primarily symmetrical rotations of the ribs around the intersecting axis of the frontal and transversal planes were found (Fig. 2). In flexion, the front tips of the upper ribs rotated to the superior direction, while the lower ribs rotated to the inferior direction, whereas in extension, the ribs exhibited inverse motion characteristics compared to flexion movement.

In lateral bending, relative motions of the ribs were particularly characterized by rotations around the intersecting axis of the sagittal and transversal planes (Fig. 3). Largest motion ranges were detected in the upper left and lower right rib cage during left lateral bending and vice versa. In case of left lateral bending, the distal rib sections tended to rotate to the superior and right direction in the upper left rib cage and to the inferior and left direction in the lower left rib cage, while the distal rib sections of the upper right rib cage rotated to the inferior and right direction and the distal rib sections of the lower right rib cage to the superior and left direction, and vice versa for right lateral bending.

In axial rotation, distinct relative motions of the ribs were especially found in the lower rib cage, which mainly consisted of rotations about the intersecting axis of the frontal and sagittal planes, but also of rotations about the intersecting axis of the sagittal and transversal planes and the intersecting axis of the frontal and transversal planes (Fig. 4). On both sides of the lower rib cage, left axial rotation caused a relative rotation of the distal rib sections to the left direction and a slight motion of the front tips to the superior direction, while the distal rib sections rotated to the superior direction on the left rib cage and to the inferior direction on the right rib cage. Right axial rotation resulted in inverse rotation characteristics, but also exhibited small motion of the front tips to the superior direction.

3.2. Relative motions of adjacent ribs

Characteristic relative motion patterns of the ribs were detected during spinal movement depending on the motion direction, showing symmetrical behaviour with regard to the sagittal plane in case of flexion/extension and inverse behaviour with regard to the sagittal plane in case of lateral bending and axial rotation (Figs. 5–7).

In flexion, a distinct compression of the anterior rib cage was found in the caudal region between rib levels 9 and 12 and particularly between 10th and 11th ribs, while the posterior rib sections were slightly (1–5%) elongated (Fig. 5). In extension, the rib cage exhibited reverse motion behaviour with the anterior rib cage section being elongated in the caudal region and the posterior section being slightly (1–7%) compressed.

In lateral bending, a distinct and almost homogeneous compression of the left rib cage was detected during left lateral bending as well as of the right rib cage during right lateral bending, whereas both the right and left rib cage were almost homogeneously elongated during left and right lateral bending, respectively (Fig. 6). Strain peaks were found in the lateral and posterolateral region, particularly in the caudal region.

In axial rotation, complex strain patterns were detected, which primarily consisted of a principal strain area running from the cranial/posterior to the caudal/anterior region, with maximum strains in the caudal/anterior region, while beyond this principal strain area reverse strains were found (Fig. 7). In this area, compression dominated on the left rib cage and elongation prevailed on the right rib cage during left axial rotation, whereas during right axial rotation, elongation was dominant on the left rib cage and compression on the right rib cage.

3.3. Bending deformation of ribs

Relative rib deformations were overall very low during thoracic spinal motion, exhibiting strain values below 1% and minimal reproducible compression or elongation behaviour, especially in lateral bending movements. Global rib deformation was primarily detected for the first rib level, where slight compression was found in flexion and slight elongation in extension. In left axial rotation, the first left rib tended to be slightly elongated and the first right rib to be slightly compressed, and vice versa for right axial rotation. Reproducible local rib deformation was detected in flexion and extension for the first three rib levels, while in flexion, mainly compression was found, whereas elongation dominated in extension, each decreasing from anterior to posterior direction. In axial rotation, slight strains were observed across the entire rib cage, which tended to increase from anterior to posterior direction for each rib. Compression was predominantly detected on the left rib cage in left axial rotation as well as on the right rib cage in right axial rotation, while the opposite side of the rib cage was mostly elongated, respectively. All strain data including maximum and minimum values can be retrieved from the supplementary material file attached to the electronic version of this article.

3.4. Rib-sternum relative motions

Complex three-dimensional motion characteristics were found between the ribs and the two sternal components dependent on

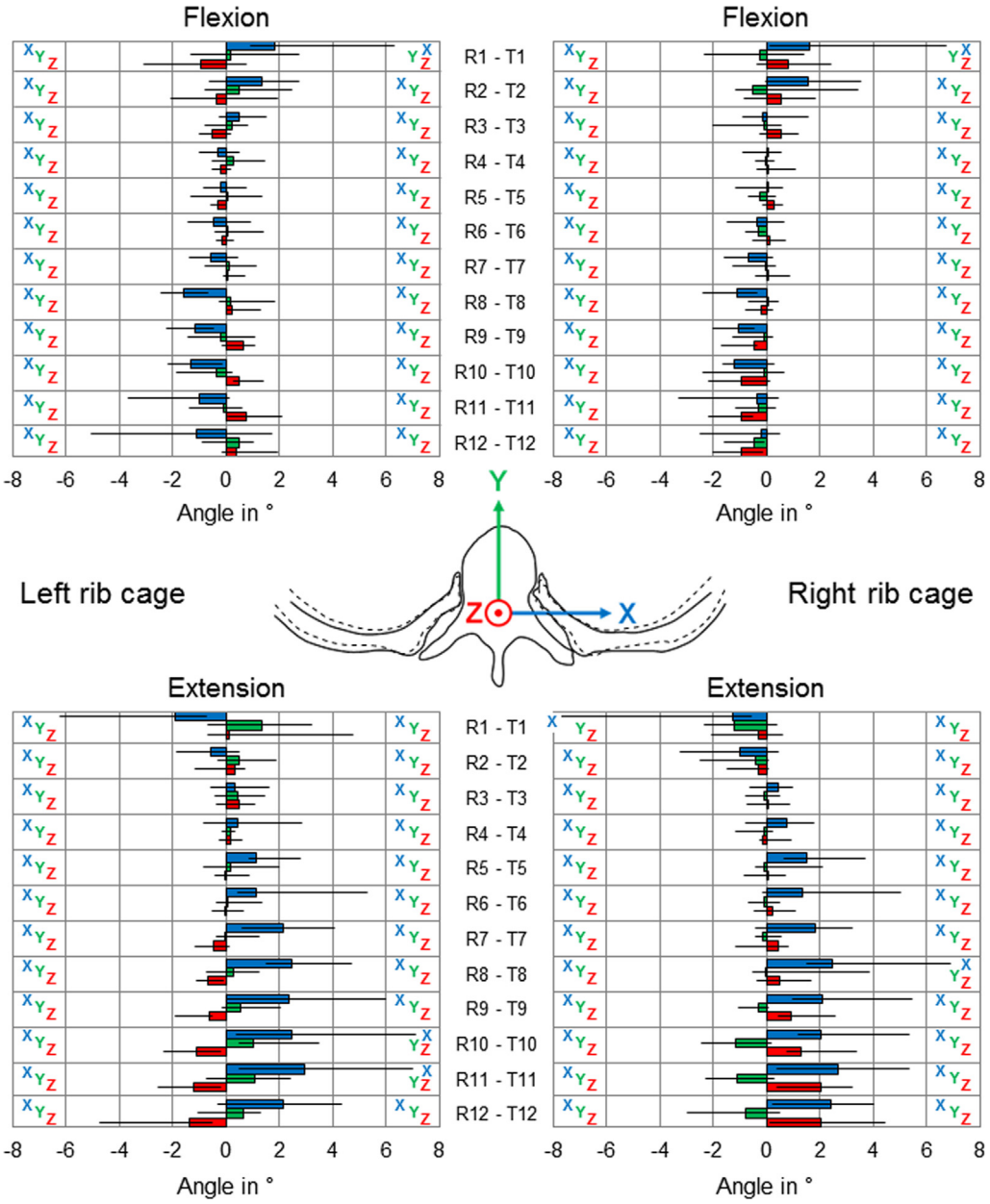

Fig. 2. Diagrams showing the 3D motion range of the ribs relative to the adjacent vertebrae in flexion/extension at full thoracic spinal loading with pure moments of 5 Nm. Data is presented as medians with ranges (n = 8). Directions of rotations around the axes of the coordinate system in the respective vertebra, as defined in the schematic drawing, follow the right-hand rule. R = Rib level, T = Thoracic vertebral level.

spinal motion planes, while motion ranges were below 2° in most cases (Fig. 8).

Motions of the first ribs relative to the upper sternum were primarily recognised as rotations around the intersecting axis of the frontal and transversal planes, resulting in a bilateral motion of the rib heads to the inferior direction (Fig. 8). Same motion was detected for the left rib head in left lateral bending and the right rib head in right lateral bending, whereas the respective opposite rib head moved to the superior direction. In axial rotation, the rib tended to rotate around the intersecting axis of the sagittal and transversal planes, with the lateral rib portions moving in inferior direction in case of the left rib in left axial rotation and the right rib in right axial rotation, while the lateral rib portions moved in superior direction on the respective opposite sides.

Compared to the relative motions between first ribs and upper sternum, generally lower and less reproducible motion ranges were detected between third ribs and lower sternum in all spinal motion planes, with exception of axial rotation, where rotations of the ribs around the intersecting axis of the frontal and sagittal planes were observed (see also Supplementary material). The left rib rotated outwards in left axial rotation, as well as the right rib in right axial rotation, whereas the respective opposite ribs rotated inwards.

3.5. Relative motions of upper and lower sternum

Motions of the upper sternum relative to the lower sternum exhibited dependency of the motion ranges from the spinal motion plane, while generally no distinct reproducible motion patterns were seen, especially in flexion/extension (see also Supplementary material). In lateral bending, the upper sternum slightly tended to rotate around the intersecting axis of the frontal and sagittal planes

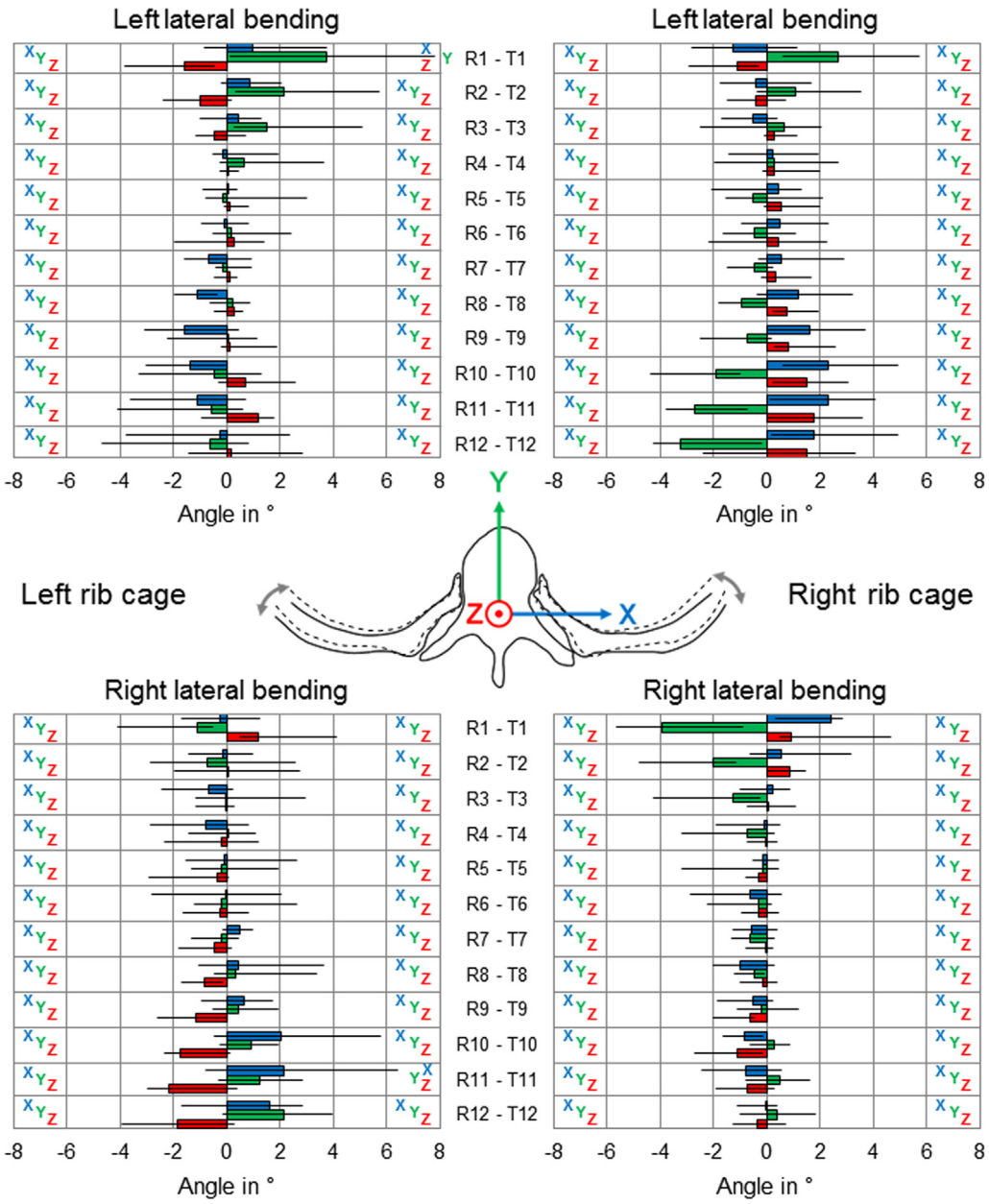

Fig. 3. Diagrams showing the 3D motion range of the ribs relative to the adjacent vertebrae in lateral bending at full thoracic spinal loading with pure moments of 5 Nm. Data is presented as medians with ranges (n = 8). Directions of rotations around the axes of the coordinate system in the respective vertebra, as defined in the schematic drawing, follow the right-hand rule. R = Rib level, T = Thoracic vertebral level.

as well as the intersecting axis of the sagittal and transversal planes, with the upper sternum rotating to the left and tilting to the right direction in left lateral bending, and vice versa in right lateral bending. In axial rotation, the upper sternum minimally tended to rotate around the intersecting axis of the frontal and sagittal planes and exhibited a distinct tendency towards a rotation around the intersecting axis of the sagittal and transversal planes. In left axial rotation, the upper sternum slightly rotated to the right and tilted to the right direction, while slightly rotating to the left and tilting to the left direction in right axial rotation.

4. Discussion

Detailed knowledge about the complex biomechanical properties of the human rib cage is essential for the accurate validation of numerical models of the thoracic spine including the entire thoracic cage, but also for the interpretation of in vitro studies investigating the thoracic spinal region with respect to the stabilizing effect of the rib cage. The present study therefore aimed to determine the kinematics and stiffness properties of all bony rib cage structures during three-dimensional thoracic spinal movements.

The results of the present study generally revealed distinct reproducible relative motions, especially in the lateral and posterior sections of the rib cage among the individual adjacent ribs as well as in the costovertebral joints. Rib-vertebrae relative motions were highest in the cranial and caudal sections in all thoracic spinal motion directions, whereas lowest relative motions were found around the segmental level T5-T6, indicating that the rib cage allows fluent transitions regarding flexibility in superior and inferior direction towards the cervical and lumbar spine while stabilizing the thoracic spine in the mid-thoracic region. This is in accordance with observations of previous in vitro studies testing

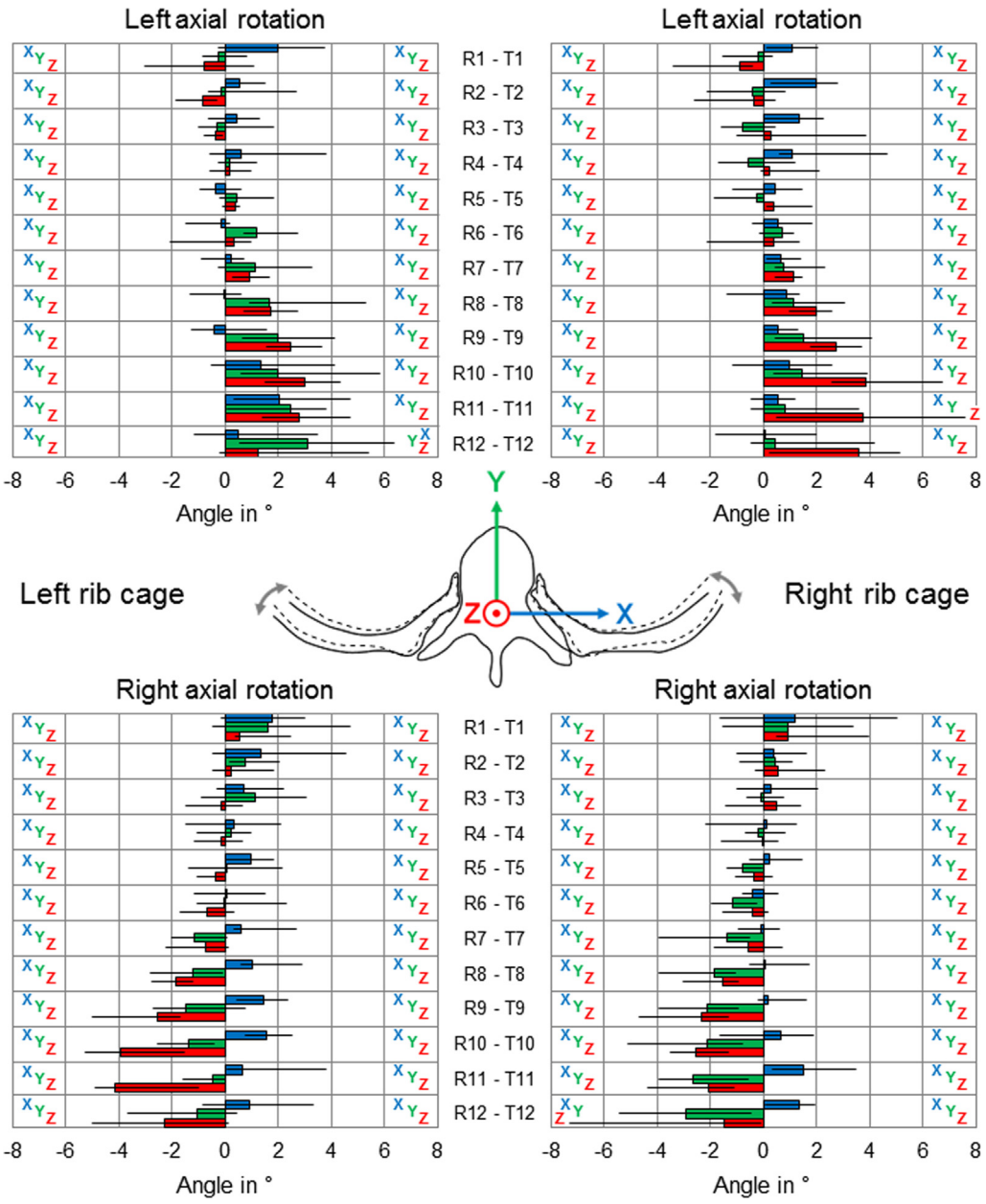

Fig. 4. Diagrams showing the 3D motion range of the ribs relative to the adjacent vertebrae in axial rotation at full thoracic spinal loading with pure moments of 5 Nm. Data is presented as medians with ranges (n = 8). Directions of rotations around the axes of the coordinate system in the respective vertebra, as defined in the schematic drawing, follow the right-hand rule. R = Rib level, T = Thoracic vertebral level.

entire rib cage specimens, where lowest spinal flexibility was found in the mid-thoracic spinal region (Liebsch et al., 2017a, 2018) and could be explained by the specific rib cage morphology, exhibiting decreasing transversal cross-sectional areas in cranial and caudal directions due to its elliptic shape in the frontal and sagittal planes.

The analysis of relative motions between the adjacent ribs exhibited distinct compressions and elongations of the intercostal spaces, particularly in the anterior caudal rib cage sections. This part of the rib cage comprises the false ribs at the rib levels 8–10, which are indirectly connected to the sternal complex via costal cartilage, as well as the floating ribs at the rib levels 11 and 12, which represent rudimentary structures and which do not have an anterior cartilaginous connection to the sternum. Therefore, it can be assumed that the deformability of the lateral rib cage section inversely correlates with the grade of costosternal connectivity.

No relevant macroscopic bending deformation was detected on the ribs during spinal loading, neither globally nor locally. Since the relative motions of all rib cage structures were distinctly higher compared to the strains on the ribs, it can be concluded that the bony structures of the rib cage are not subjected to substantial deformation during physiological motions of the spine, while its structures exhibit considerable relative kinematics due to the respective connecting joints. Furthermore, the existence of costal cartilage can be seen as a compromise in creating stability and flexibility for the rib cage and the thoracic spine.

Previous in vitro studies investigated motion ranges of the costovertebral joints measuring rib deflections and joint stiffness values in different motion planes using experimental setups where single thoracic spinal motion segments were clamped and the ribs were loaded by certain weights or by defined pushing via lever arms under load cell control. These studies found that motion

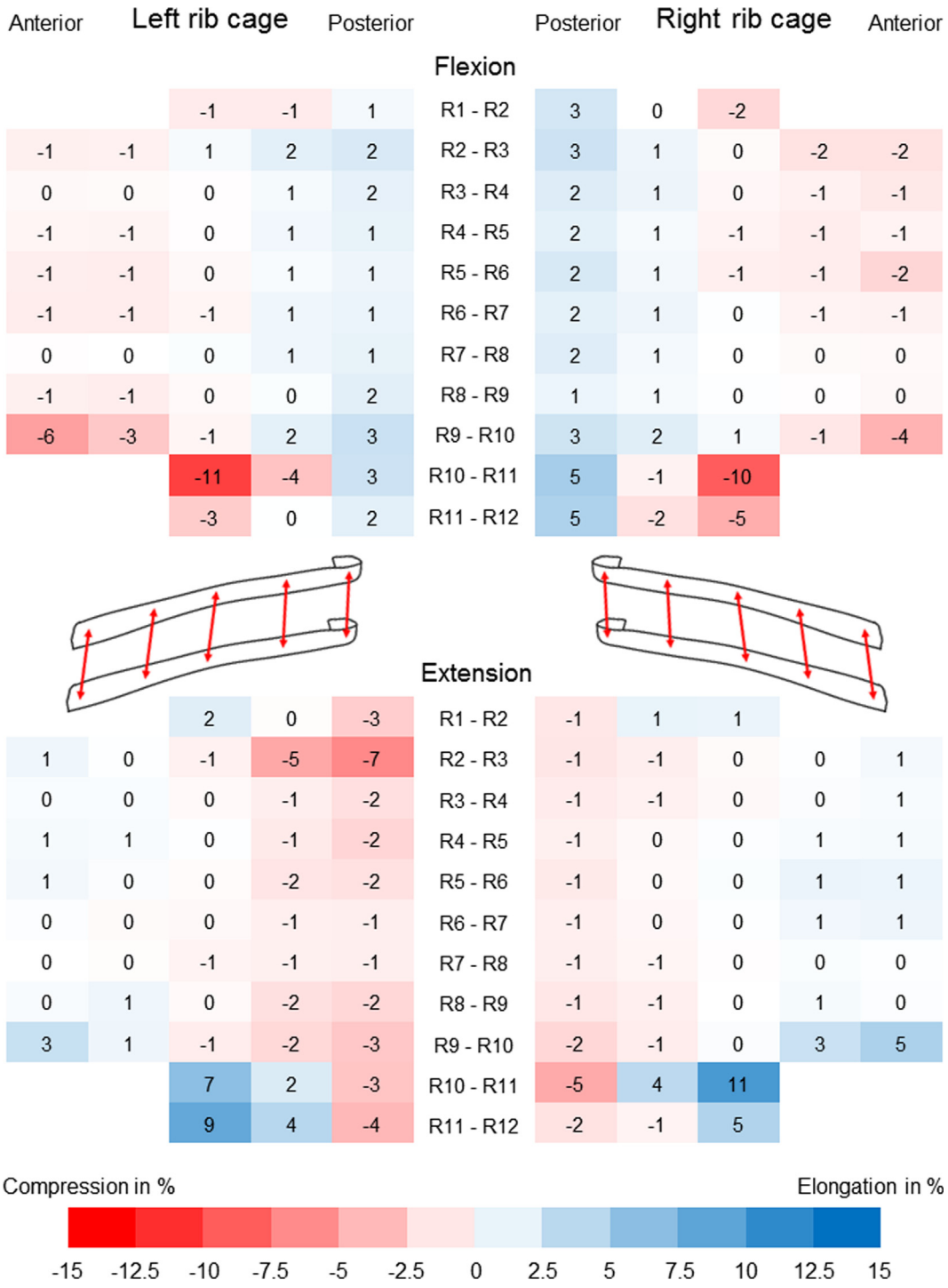

Fig. 5. Heat maps illustrating the strains between the single ribs along their curvature in flexion/extension at full thoracic spinal loading with pure moments of 5 Nm. Data is presented as medians (n = 8). R = Rib level.

range and flexibility of the costovertebral joints are by far highest in case of rotation around the axis formed of the connection between the articular surfaces of the costovertebral and costotransverse joints (Schultz et al., 1974; Lemosse et al., 1998; Duprey et al., 2010), while the overall joint stiffness tended to decrease in caudal direction of the rib cage (Duprey et al., 2010). This motion and stiffness pattern can be explained by the specific morphology and attachment points of the costovertebral ligaments (Schlager et al., 2018), allowing lifting and sinking of the rib cage during respiration and stabilisation of the spine at the same time. Through inhalation, the ribs are lifted by muscle forces to increase the intra-thoracic volume. In vivo studies investigating the respiration process showed by means of CT reconstruction that the main motions are performed around the same axes of rotations as found in previous in vitro studies (Beyer et al., 2014, 2015, 2016, 2017). Due to the decreasing length of the thoracic spinal transverse processes in caudal direction, the angles of the rotation axes within the transversal plane alter across the segmental levels, exhibiting an average value of 45° to the frontal plane (Wilson et al., 2001). In the upper rib cage, where the angle is slightly reduced, a joint

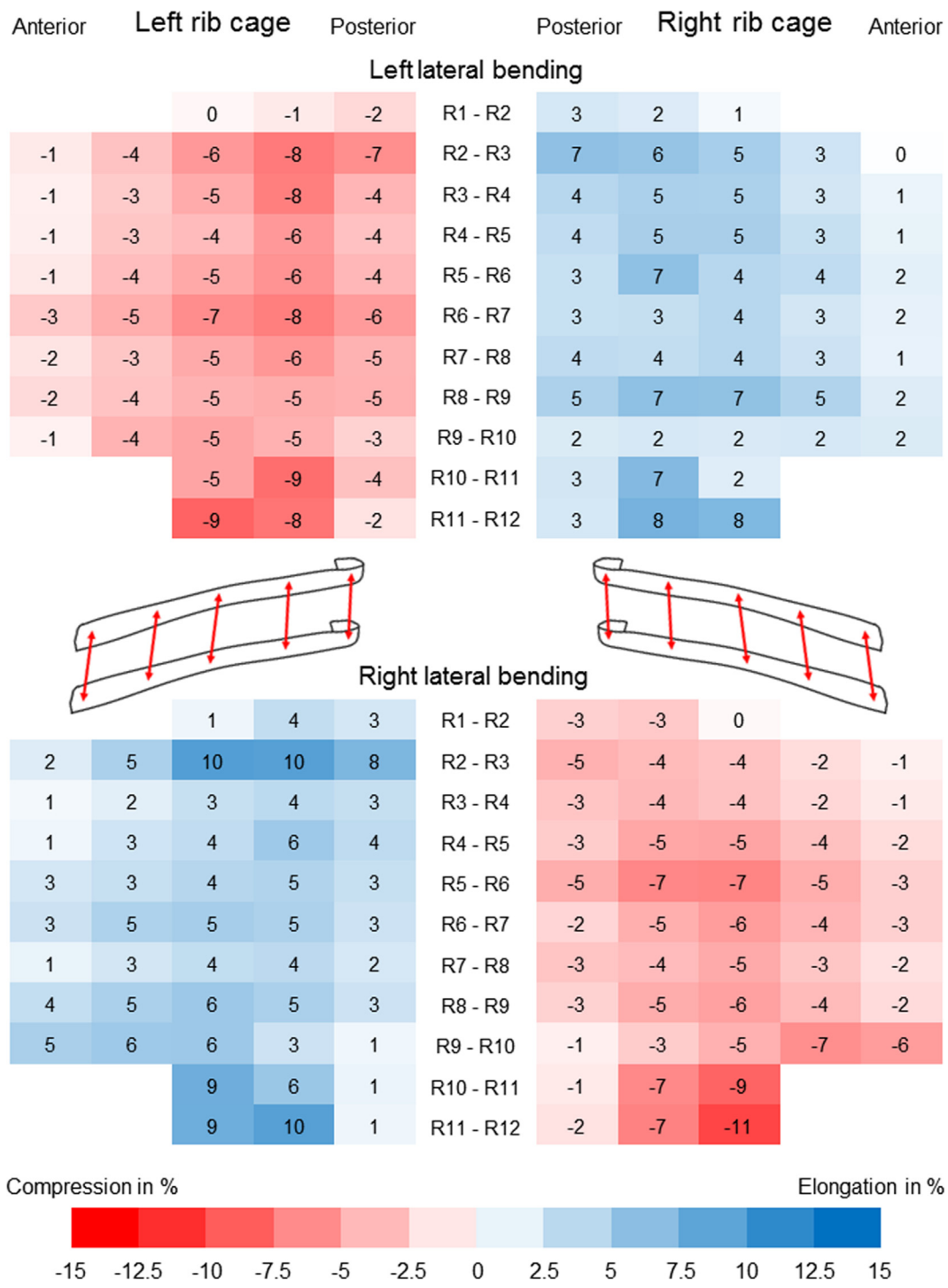

Fig. 6. Heat maps illustrating the strains between the single ribs along their curvature in lateral bending at full thoracic spinal loading with pure moments of 5 Nm. Data is presented as medians (n = 8). R = Rib level.

rotation is produced, which induces lifting of the rib front tip to increase the anteroposterior rib cage diameter, also referred to as pump handle motion (Wilson et al., 1987). In the lower rib cage, where the angle is higher than 45°, the lateral sections of the ribs are lifted to increase the transversal rib cage diameter, also described as bucket handle motion (Wilson et al., 1987). In the present study, it was further shown that relative motions between ribs and vertebrae mainly arise in the cranial and caudal fourths of the rib cage during thoracic spinal motion.

In future studies, strains of the rib and costal cartilage surfaces should be additionally investigated using optical strain measurement devices or strain gauges to analyse the microscopic deformation of the ribs during spinal motion. In vitro simulations of the respiration process, the intraabdominal and intrapleural pressure, or muscle activity during upright standing, which presumably affect the stiffness and kinematic parameters, are challenging from a technical point of view and should be performed in silico using validated numerical models. In the present study, it was tried

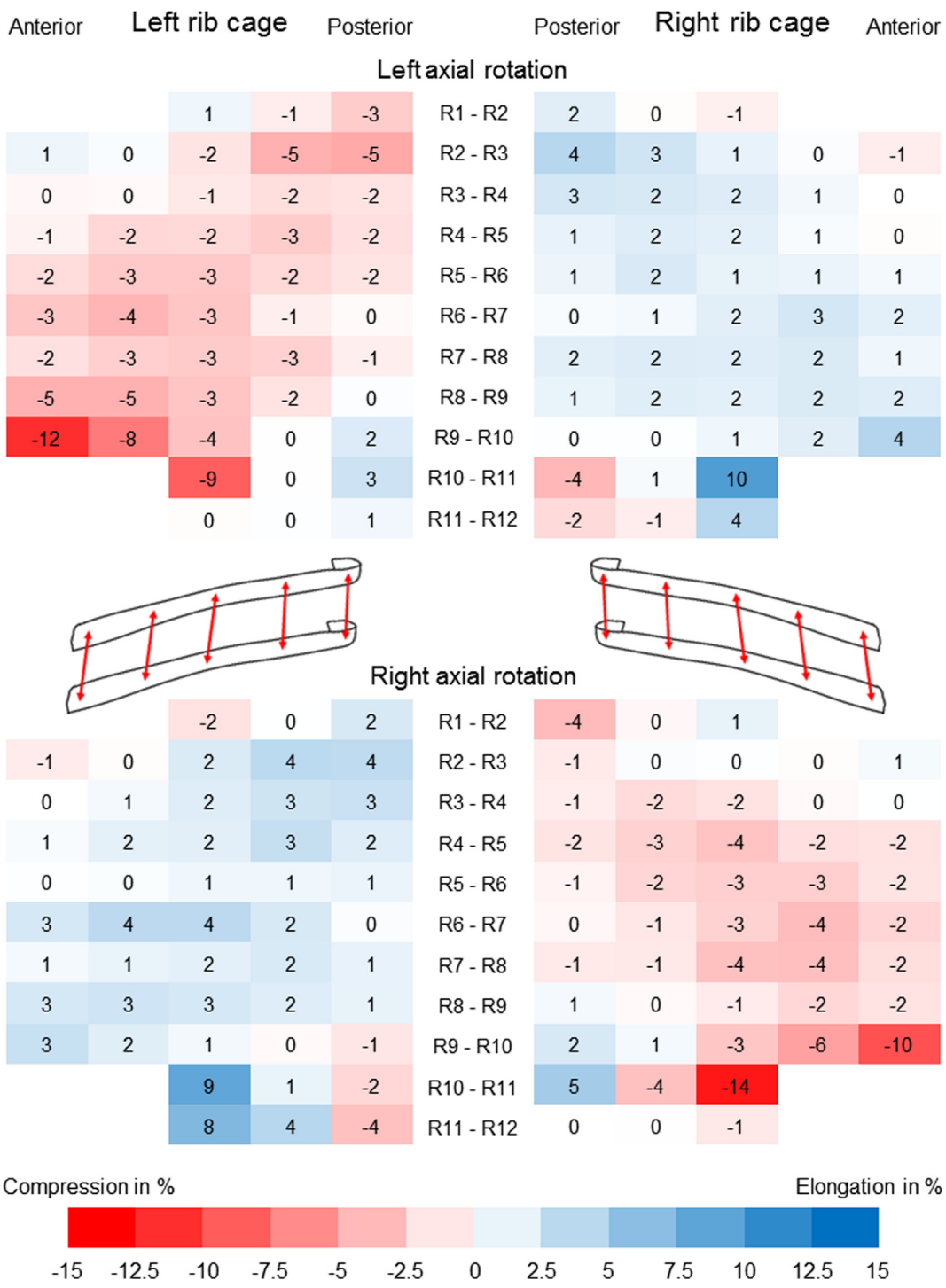

Fig. 7. Heat maps illustrating the strains between the single ribs along their curvature in axial rotation at full thoracic spinal loading with pure moments of 5 Nm. Data is presented as medians (n = 8). R = Rib level.

to simulate rib cage motion as physiologically as possible, for instance by preserving the intercostal muscles, since they were shown to absorb tension forces (Liebsch et al., 2017a). Spinal loading by means of pure moments, as used in the present study, however, does not simulate physiological loading, but was applied to create better comparability among the results compared to the simulation of specific muscle forces. Nevertheless, the used methodology represents the current state of research and the results of this study can be of value regarding the development and optimization of thoracic spinal and rib cage implants or the interpretation of clinical findings regarding thoracic flexibility.

The findings of the present study should be understood with regard to the specific boundary conditions, particularly in the context of validating numerical models. Considering this, the data generated within the present study can be used to accurately validate numerical models of the thoracic spine including the entire rib cage.

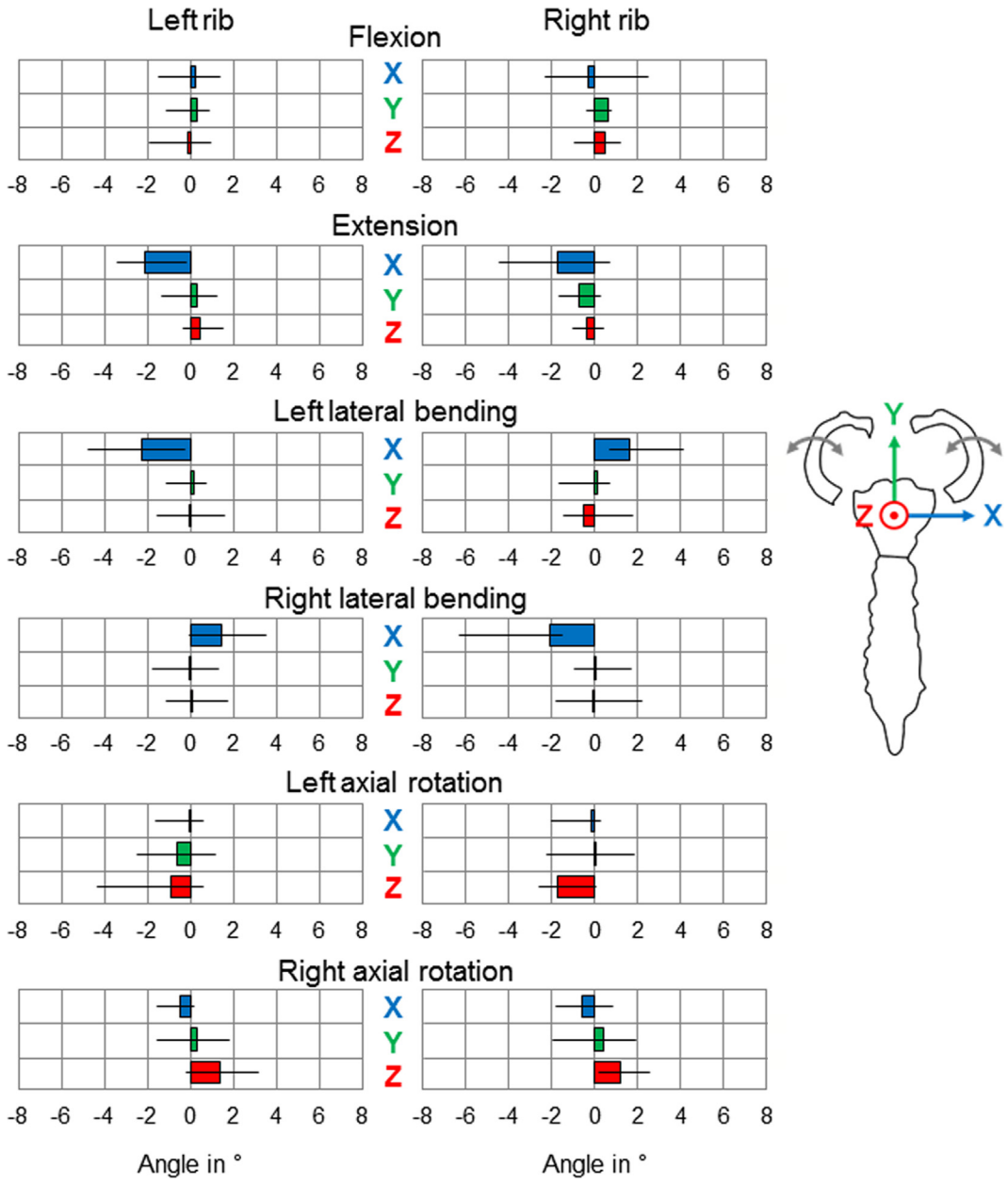

Fig. 8. Diagrams showing the 3D motion range of the 1st ribs relative to the upper sternum at full thoracic spinal loading with pure moments of 5 Nm. Data is presented as medians with ranges (n = 8). Directions of rotations around the axes of the coordinate system in the upper sternum, as defined in the schematic drawing, follow the right-hand rule.

Declaration of Competing Interest

The authors of this study declare to have no conflict of interest to disclose.

Acknowledgments

This study was supported by the German Research Foundation (DFG, Project WI 1352/20-2). The funding agency had no influence on study design, data collection, analysis, or interpretation, manuscript preparation, and the decision to submit the manuscript for publication.

Appendix A. Supplementary material

Supplementary data to this article can be found online at https://doi.org/10.1016/j.jbiomech.2019.07.041.

References

Beyer, B., Feipel, V., Sholukha, V., Cheze, L., Van Sint Jan, S., 2017. In-vivo analysis of sternal angle, sternal and sternocostal kinematics in supine humans during breathing. J. Biomech. 64, 32–40.
Beyer, B., Sholukha, V., Dugailly, P.M., Rooze, M., Moiseev, F., Feipel, V., Van Sint Jan, S., 2014. In vivo thorax 3D modelling from costovertebral joint complex kinematics. Clin. Biomech. 29 (4), 434–438.
Beyer, B., Sholukha, V., Salvia, P., Rooze, M., Feipel, V., Van Sint Jan, S., 2015. Effect of anatomical landmark perturbation on mean helical axis parameters of in vivo upper costovertebral joints. J. Biomech. 48 (3), 534–538.
Beyer, B., Van Sint Jan, S., Cheze, L., Sholukha, V., Feipel, V., 2016. Relationship between costovertebral joint kinematics and lung volume in supine humans. Respir. Physiol. Neurobiol. 232, 57–65.
Duprey, S., Subit, D., Guillemot, H., Kent, R.W., 2010. Biomechanical properties of the costovertebral joint. Med. Eng. Phys. 32 (2), 222–227.
Kindig, M.W., Lau, A.G., Forman, J.L., Kent, R.W., 2010. Structural response of cadaveric ribcages under a localized loading: stiffness and kinematic trends. Stapp Car Crash J. 54, 337–380.
Lemosse, D., Le Rue, O., Diop, A., Skalli, W., Marec, P., Lavaste, F., 1998. Characterization of the mechanical behaviour parameters of the costo-vertebral joint. Eur. Spine J. 7 (1), 16–23.

Liebsch, C., Graf, N., Appelt, K., Wilke, H.J., 2017a. The rib cage stabilizes the human thoracic spine: An in vitro study using stepwise reduction of rib cage structures. PLoS One 12, (6) e0178733.

Liebsch, C., Graf, N., Wilke, H.J., 2017b. EUROSPINE 2016 FULL PAPER AWARD: Wire cerclage can restore the stability of the thoracic spine after median sternotomy: an in vitro study with entire rib cage specimens. Eur. Spine J. 26 (5), 1401–1407.

Liebsch, C., Graf, N., Wilke, H.J., 2018. The effect of follower load on the intersegmental coupled motion characteristics of the human thoracic spine: An in vitro study using entire rib cage specimens. J. Biomech. 78, 36–44.

Mannen, E.M., Anderson, J.T., Arnold, P.M., Friis, E.A., 2015a. Mechanical analysis of the human cadaveric thoracic spine with intact rib cage. J. Biomech. 48 (10), 2060–2066.

Mannen, E.M., Anderson, J.T., Arnold, P.M., Friis, E.A., 2015b. Mechanical Contribution of the Rib Cage in the Human Cadaveric Thoracic Spine. Spine 40 (13), E760–E766.

Schlager, B., Niemeyer, F., Liebsch, C., Galbusera, F., Boettinger, J., Vogele, D., Wilke, H.J., 2018. Influence of morphology and material properties on the range of motion of the costovertebral joint - a probabilistic finite element analysis. Comput. Methods Biomech. Biomed. Engin. 21 (14), 731–739.

Schultz, A.B., Benson, D.R., Hirsch, C., 1974. Force-deformation properties of human costo-sternal and costo-vertebral articulations. J. Biomech. 7 (3), 311–318.

Watkins 4th, R., Watkins 3rd, R., Williams, L., Ahlbrand, S., Garcia, R., Karamanian, A., Sharp, L., Vo, C., Hedman, T., 2005. Stability provided by the sternum and rib cage in the thoracic spine. Spine 30 (11), 1283–1286.

Wilke, H.J., Claes, L., Schmitt, H., Wolf, S., 1994. A universal spine tester for in vitro experiments with muscle force simulation. Eur. Spine J. 3 (2), 91–97.

Wilke, H.J., Wenger, K., Claes, L., 1998. Testing criteria for spinal implants: recommendations for the standardization of in vitro stability testing of spinal implants. Eur. Spine J. 7 (2), 148–154.

Wilson, T.A., Legrand, A., Gevenois, P.A., De Troyer, A., 2001. Respiratory effects of the external and internal intercostal muscles in humans. J. Physiol. 530 (2), 319–330.

Wilson, T.A., Rehder, K., Krayer, S., Hoffman, E.A., Whitney, C.G., Rodarte, J.R., 1987. Geometry and respiratory displacement of human ribs. J. Appl. Physiol. 62 (5), 1872–1877.